Dispatch optimization of battery energy storage systems considering degradation effects and capacity inhomogeneities in second life batteries

Melina Graner[1,2], Vivek Teja Tanjavooru[2], Andreas Jossen[1], Holger Hesse[2]

[1]*Technical University of Munich, School of Engineering and Design, Department of Energy and Process Engineering, Chair for Electrical Energy Storage Technology, Munich, Germany*
[2]*Kempten University of Applied Sciences, Department of Mechanical Engineering, Institute for Energy and Propulsion Technology (IEAT), Kempten, Germany*
Correspondence author. Email: melina.graner@hs-kempten.de

ABSTRACT

The performance of battery energy storage systems (BESS) along their lifetime is significantly influenced by their degradation. The rate of degradation depends on stress factors such as the State-of-Charge, charge-discharge-rate, and depth of cycle, but evolves differently for every individual battery. Batteries with differences in capacity and or State-of-Health may diverge further apart when cycled evenly causing further inhomogeneities. BESS can also consist of heterogeneous sub-units if Second-Life-Batteries with reduced capacity and or State-of-Health are integrated in the system. In order to minimize the overall system aging effects those variances can be balanced with an according operation strategy. This contribution presents a model predictive control (MPC) framework that helps to solve optimization problems regarding the power split within heterogeneous BESS-models. An exemplary 2-string-battery model is used to represent batteries with different characteristics and it contains cycle and calendar aging mechanisms. In our case one of the strings is preaged. The MPC framework combines aging estimation and operation optimization by using a commercial solver. It iterates over a given profile and predicts the optimal power split between the heterogeneous strings. By defining the system‘s total minimal capacity loss as an objective function, the optimizer achieves to minimize the BESS-model‘s overall capacity-loss during operation. The simulation reveals that while the new string ages by 1.23 %, the preaged string will lose 0.258 % State-of-Health within the 21-day timeframe investigated.

Keywords: *Battery System, Stationary Energy Storage, Linear Optimization, Second Life, Capacity Loss, State of Health*

1. INTRODUCTION

The globally installed capacity of stationary battery energy storage systems (BESS) has increased steadily in recent years as they are considered as a critical component of the energy transition. BESS serve multiple use cases and are installed in different applications. In behind-the-meter applications such as peak shaving and self-consumption increase, they help to optimize electricity consumption and tariffs for end-users whereas front-of-the-meter applications such as frequency regulation and energy trading are investment cases with BESS generating revenue in the energy and power markets. Battery development has received significant attention from the industrial and scientific communities in recent years and lithium-ion-batteries (LIB) nowadays are the leading battery technology. [1], [2], [3]

1.1. Literature review

Batteries are subject to degradation due to multiple cell-internal aging effects that cause a decrease in cell capacity and an increase of the cell’s internal resistance. This degradation depends on internal factors (such as cell design and material parameters) but also on external influence factors such as the batteries’ previous age, the operator’s usage patterns (charge-discharge schedule) or environmental exposure (e.g. ambient temperature) [4]. Cell level aging mechanisms have been studied intensively during the last years in research and industry, focussing on the influence of different cycling and storage conditions on battery behaviour. [5], [6]

Aging mechanisms on system level depend on the cells’ individual aging behaviour and affect the remaining useful life (RUL) and the BESS’s economic viability [7]. Several approaches for the determination

P. Droege and L. Quint (eds.), *Proceedings of the International Renewable Energy Storage and Systems Conference (IRES 2023)*, Atlantis Highlights in Engineering 32,
https://doi.org/10.2991/978-94-6463-455-6_4

Abbreviations

BESS	Battery energy storage system
C-rate	Charge–discharge rate
DOC	Depth of Cycle
EV	Electric vehicles
FEC	Full equivalent cycle
LIB	Lithium-ion-batteries
LFP	Lithium-iron-phosphate
MILP	Mixed-integer-linear-programming
MPC	Model predictive control
RUL	Frequency containment reserve
RUL	Remaining useful life
SLB	Second life batteries
SOC	State-of-Charge
SOH	State-of-Health

of operation strategies were developed, some of them considering the aging costs for higher profits over the BESS lifetime. [8], [9], [10] The capacity of battery systems consisting of a various number of connected cells is determined by the weakest cell within the series connection, which in consequence also specifies the lifetime of the system [11]. In order to closely investigate and optimize the performance of an entire battery pack, the influence of cell-to-cell inhomogeneities needs to be considered. Inhomogeneities within battery systems can be variations in resistance, initial capacity and aging rate caused by tolerances in the cell production. Additionally there are temperature inhomogeneities caused by cooling systems within the battery system as well as electric inhomogeneities [12]. The inhomogeneities occur with smaller spread at the begin-of-life of batteries but their influence may increase with bigger spreads along the usage life. The relevance of increasing spreads and variances needs to be taken especially into account when it comes to integrating second life batteries (SLB) into BESS.

The reuse of retired batteries from electric vehicles (EV) has gained increasing attention from academics and industry in the past few years. Transferring batteries into a second-life after they no longer meet the EV performance standards (which typically means maintaining 70-80 % of total usable capacity) is part of a circular end-of-life strategy that supports the sustainability of battery technology. [13], [14] Compared to battery recycling for a secondary raw material supply, reuse is more environmentally attractive from a holistic life cycle perspective. Cascading the usage-lifetime of batteries is considered by both regulatory and industrial bodies, for example in the European Commission's directive that strengthens sustainability rules for batteries and waste batteries [15]. The concept of reuse of SLB in BESS has the potential to optimize costs and resource utilization. Multiple studies, simulations and project reviews investigated and proved the technical and economic viability of SLB in

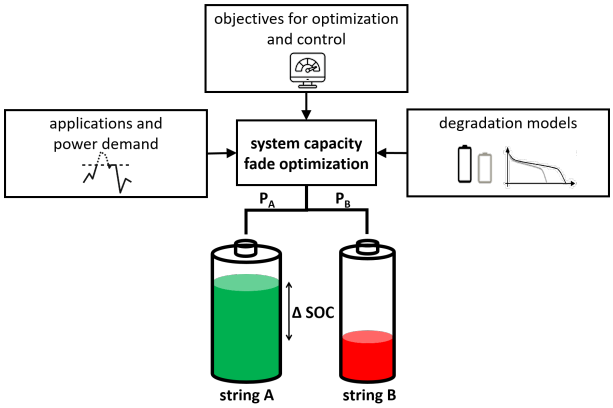

Figure 1 Methodology of developing the power allocation P_A and P_B of a 2-string battery model with capacity fade optimization: the optimal operation strategy is evaluated based on previously investigated aging mechanisms and semi-empirical degradation models, user-defined objective functions, and an application-specific power demand profile. The BESS model itself consists of two inhomogeneous strings A and B with different initial State-of-Charge (bucket model based SOC) and SOH.

BESS. [16], [17], [18] The development of efficient control strategies focussing on BESS that consist of SLB and considering their different aging behaviour (compared to BESS consisting of new batteries) received less scientific attention so far. As the spread of previous mentioned characteristics increases over lifetime, SLB show not only a reduced State-of-Health (SOH). The aging behaviour of sub-units within battery systems is inhomogeneous as well and as it affects the RUL and the BESS's economic viability, control strategies need to balance the power split between heterogeneous sub-units accordingly. There is a gap in the existing literature that links aging aware control strategies of BESS with the challenge of heterogeneity in BESS which this contribution aims to bridge. In particular it takes inhomogeneities in BESS that incorporate SLB into account. Depending on the topology of cell-to-cell interconnections and module-to-system configuration, there are degrees of freedom for the energy management system to control the dispatch of sub-units of the system individually. This contribution intends to use these degrees of freedom to operate a BESS efficiently despite different aging states of sub-units and to compensate capacity differences. An optimization framework considering calendar and cycle aging is used to determine and minimize the overall capacity fade of a BESS-model during operation. The framework will also be applied and investigated in the context of SLB with different levels of capacity or SOH.

1.2. Structure and contributions

Fig. 1 shows the methodology of developing the framework for the system lifetime optimization. The

following section 2 first describes the proposed model predictive control (MPC) framework (section 2.1) and the corresponding demand profile (section 2.2). The previously investigated and incorporated aging mechanisms and semi-empirical degradation models, as well as the objectives for the optimization are presented in section 2.3. In the subsequent case study in section 3 the functionality of the MPC framework is showcased (section 3.2) for a specific parameter set (presented in section 3.1). The simulation results for the combination of two heterogeneous battery strings are discussed in section 3.3. We summarize our main contributions as follows:

- empirical battery degradation model integrated into a multi-string optimization framework
- capturing of non-linear behaviour in optimization routines
- case study on inhomogeneous batteries shows performance of the algorithms with the aim to lower the overall system's capacity fade and proves the capability to equilibrate degradation effects.

2. DEGRADATION AWARE MPC STRATEGIES

Fig. 2 shows the developed MPC framework. The optimization model with its structure and constraints is a model of an exemplary BESS and should represent its functionality including its expected aging behaviour.

2.1. MPC Framework

The framework uses model predictive control to optimize the power split in the heterogeneous two-battery string system. The optimization problem itself aims for minimal system capacity loss when distributing the power among the two strings. MPC is based on a repeated optimization of a mathematical system model that is used to optimize the battery's future charge and discharge behaviour for the selected prediction horizon

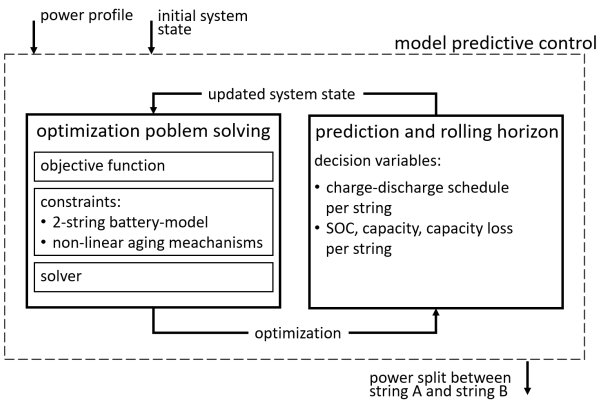

Figure 2 Depiction of the proposed MPC framework for developing overall lifetime extending power split strategies for inhomogeneous BESS models.

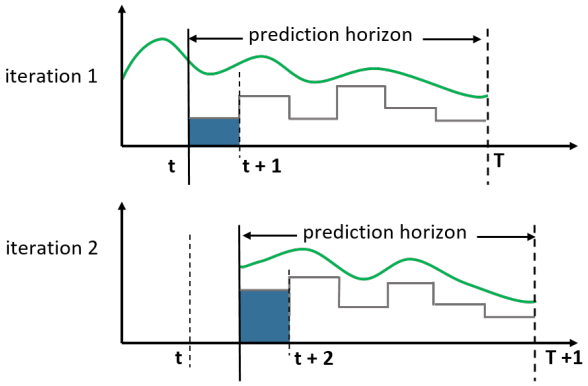

Figure 3 Rolling horizon principle used in the MPC framework. The optimizer aims to meet the forecasted demand profile (green) and predicts the optimal charge-discharge schedule for this prediction horizon (grey). Only the first bit of the output is passed back to the optimizer (control horizon in blue).

$t_{\text{prediction}}$. The optimizer iterates over the input profile in a rolling horizon manner (see Fig. 3) and then performs the computation on each prediction horizon. Only the first bit of the final optimized output trajectory of each iteration is executed (control horizon t_{control}) and the relevant MPC state values, that represent the new BESS state after these n timesteps, are handed back to the optimization model. They characterize the updated system state for solving the next prediction horizon. That way the iterations roll forward in time covering the entire input power profile while keeping the computational cast at manageable levels (see section 2.3).

2.2. Input power profile

As an input profile the reference FCR profile (frequency containment reserve) from Kucevic et al. in [19] is used and averaged to a resolution of Δt = 15 min. The simulation case study uses the first 21 days of the reference profile. The FCR power demand profile is shown in Fig. 4. The profile shows a characteristic low amplitude and high operation frequency for the FCR operation, demanding sub-average power from the batteries (in relation to other applications). The expected number of full equivalent cycles is low in combination with a small depth of discharge. Any other profile can be passed to the MPC framework as an input profile. It is compatible to different applications and different profile lengths. The latter having a linear correlation with the computation time.

2.3. Optimization model

The optimization problem is formulated within the objective function (Eq. 1)

Minimize:

$$\sum_{t=0}^{n} \text{capacity\_loss}_A(t) + \sum_{t=0}^{n} \text{capacity\_loss}_B(t) \quad (1)$$

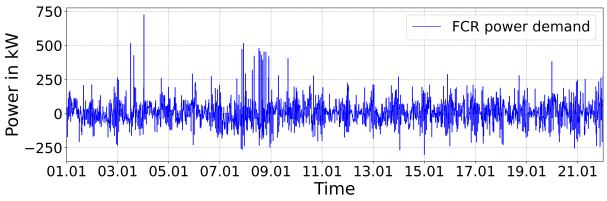

Figure 4 The FCR power demand profile that is used as an input profile for the MPC framework in this contribution.

and is modelled with mixed-integer-linear-programming (MILP). The two-string-battery model itself is characterized by the variables and constraints defining its working principle. For every prediction horizon the system computes the State-of-Charge (bucket model based SOC) considering the bi-directional power flow in each string including the corresponding inverter losses and maintaining the user defined safety-limits of 10 % and 90 % SOC. Furthermore, the constraints ensure the throughput of all the grid power and the consideration of capacity losses caused by cycle and calendar aging. The originally non-linear calendar and cyclic degradation models are formulated as constraints with the help of several auxiliary variables. This results in a non-linear estimation model for the empirically determined aging functions (Eq. 2 and 3) .

$$Q_{\text{loss, cal}}(\%) = k_{\text{temp, cal}} \cdot k_{\text{SOC}} \cdot \sqrt{t} \tag{2}$$

$$Q_{\text{loss, cyc}}(\%) = k_{\text{temp, cyc}} \cdot k_{\text{C-rate}} \cdot k_{\text{DOC}} \cdot \sqrt{\text{FEC}} \tag{3}$$

The Eq. 2 and 3 express the development of the capacity loss dependent on temperature, SOC and lifetime for calendar aging and on temperature, C-rate (charge–discharge rate), Depth of Cycle (DOC) and the number of full equivalent cycles (FEC) for cycle aging. The aging mechanisms may vary for different battery types and chemistries. For the sake of simplicity, in this contribution we confine ourselves to the same lithium-iron-phosphate (LFP) model for both strings. The relevant decision variables for the model are

- power, charge and discharge power and energy throughput for each string
- SOC for each string
- current remaining capacity and lumped capacity loss for each string.

The stress factors k_{SOC}, $k_{\text{C-rate}}$ and k_{DOC} are calculated depending on the variables SOC, DOC and C-rate. The SOC is obtained as an output value from the optimization and is further used to determine the variables DOC and C-rate. The interdependence of those variables and respectively of the optimization variables capacity_loss$_A(t)$ and capacity_loss$_B(t)$ (within the objective function) increases the complexity of the optimization problem. To adapt Eq. 2 and 3 to varying external stress factors, the concept of virtual time (t_{virtual}) and virtual FEC (FEC_{virtual}) from Naumann et al. [20], [21] is implemented. The virtual time is the time that would have been needed to pass to account for the total past calendar capacity loss under the present stress factors. Same principle applies for the virtual FEC, which is the number of full equivalent cycles that would have been needed to pass to account for the total past cyclic capacity loss under the present stress factors.

In the original model by Naumann et al. $k_{\text{temp, cal}}$ and $k_{\text{temp, cyc}}$ describe the dependence of capacity loss on temperature. In the simulations conducted herein, a constant temperature is set, in line with the sub-average load conditions imposed by FCR operation and a well operating heating, ventilation, and air conditioning system. We assume a constant temperature of 25°C. Therefore $k_{\text{temp, cal}}$ and $k_{\text{temp, cyc}}$ are constants in this model.

3. SIMULATION CASE STUDY

In this chapter, we present and discuss the simulation results we obtained with the earlier proposed MPC simulation framework. In section 3.1 we describe the parameter set for the exemplary simulation case study. Section 3.2 shows the simulation results which are evaluated in section 3.3.

In the following, the optimization model uses a prediction horizon $t_{\text{prediction}}$ of 4 hours, with a timestep width Δt of 15 min. The optimization is called at every timestep n within $t_{\text{prediction}}$ (n = 16). The commercial solver Gurobi Optimizer is used for solving the optimization model in this case study. Note that due to the quadratic and cubic aging functions the resulting optimization problem is non-linear and the constraints require a MILP solver. The simulation results described in the following sections are obtained running the simulation on a laptop with an Intel core i7-8565U CPU and 16 GB RAM. Computing the presented simulation requires approximately 24 hours with the current structure of the MPC framework.

3.1. Simulation parameter set

The optimization problem in this simulation case study uses the inputs shown in Table 1. As mentioned before in section 2.2 the input profile in this case study is a part of the standard battery energy storage system FCR profile (the first 21 days). The objective function is to minimize the $total\ system's\ capacity\ loss$ (sum of the capacity losses of string A and string B over the whole simulation time, see Eq. 2). The aging functions include the determination of capacity loss for cycle and calendar aging based on Eq. 2 and 3. Both strings are different in their initial state, thus representing the heterogeneity of the system. The initial state for string A (new string, colored green in the figures) is a starting SOC of 90 % and a SOH of 100 % indicating that this string is at the begin of its 1st life. The string B (second life string, colored red in the figures) represents a preaged subunit with a starting SOH of 85 % (indicating that it

is in second life operation) and a lower SOC of 40 %. Both strings have a nameplate capacity of 6000 kWh. For string A, having a SOH of 100 %, the nameplate capacity is the initial starting capacity for the simulation. The initial simulation capacity of string B is only 5100 kWh due to the reduced SOH of 85 %.

3.2. *Simulation optimization results*

Fig. 5 and 6 show the simulation results regarding SOC and capacity for an optimization problem using the inputs from Table 1. The optimization framework obtains a power split between both strings which results in the minimal total capacity loss of the whole system.

Fig. 5 shows the SOCs of the power split strategy the MPC framework derived. The SOCs of both strings intersect after roughly four days and the SOC of string B which started at 40 % on the long run oscillates around 75 %. The SOC of string A rapidly falls from 90 % within the first three days down to 65 % and then oscillates around 70 % on the long run. The difference in SOC decreases to a value of roughly 5 % on the long run. The SOC of the new string A is driven to a lower level in order to minimize the SOC dependent capacity loss of the new battery at the cost of a higher SOC level for string B: string B has to cope with a higher level of SOC in order to fulfil the demand profile. If the simulation instead was run with a different parameter set of two new strings with a SOH of 100 %, the SOC of both strings would converge and oscillate around the same SOC level of 67 % on the long run.

Fig. 6 shows the decreasing capacity in kWh for both strings A and B. String A loses more capacity than string B due to the higher initial SOH. The shape of capacity A reflects the strong influence of calendar capacity loss. The near square-root dependency of lifetime and the influence of a high SOC level cause the higher capacity loss in string A. If the starting capacities of both strings were considered their nominal capacity, the loss in SOH at the end of the 21-day profile would be 1.23 % for string A and 0.258 % for string B.

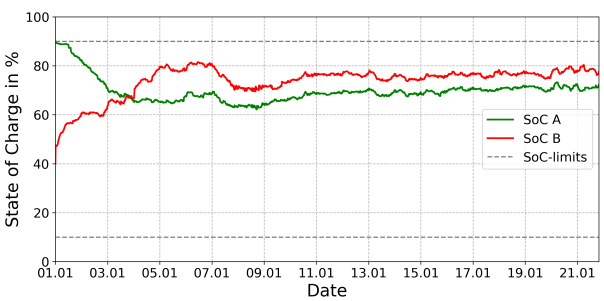

Figure 5 SOC per timestep (resolution 15 min) for the two strings A and B for a 21-day FCR profile. The y-axis shows the SOC in percentage and the x-axis notes the dates for the 21-day FCR profile (from 1st of January to the 21st of January). The SOC boundaries of of 10 % and 90 % are plotted in grey.

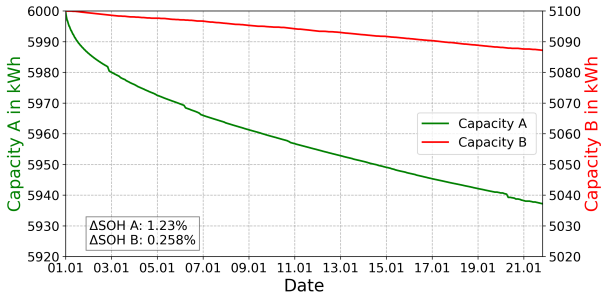

Figure 6 Capacity per timestep (resolution 15 min) for the two strings A (left y-axis) and B (right y-axis) for a 21-day FCR profile. The y-axes show the capacity in kWh and the x-axis notes the dates for the 21-day FCR profile (from 1st of January to the 21st of January).

The aging behaviour in both strings is dominated by calendar aging. In string A the calendar aging accounts for 89.3 % of total aging, whereas cycle aging accounts for only 10.7 %. In string B the capacity loss is much lower compared to string A but the influence of calendar ageing is even greater with 98.7 % of total aging, whereas cycle aging accounts for only 1.3 %.

3.3. *Discussion of results*

The simulation results shown in Fig. 5 and 6 are representative for the LIB-characteristic non-linear aging behaviour. For LFP batteries the aging behaviour is dominated by calendar aging. The development of the capacities matches the correlation of stress factors in the calendar capacity loss function (Eq. 2). Especially the near square-root dependency of calendar lifetime becomes clear when comparing the curves of capacity A and capacity B. The capacity of the preaged string B decreases with a much smaller gradient than string A, meaning the capacity loss per timestep is much higher for string A than for string B, especially in the first timesteps. Therefore the power split gets adjusted accordingly: the preaged string B is pushed towards a higher SOC than string A, in order to minimize the SOC dependent capacity loss.

The simulation trial underlines the capability of the MPC framework to handle the non-linear constraints (caused by the equations for capacity loss). The result underlines, that inhomogeneous batteries should be dispatched with unit-specific power control, allowing to adapt the string individual power setpoints and to minimize the overall aging associated capacity loss. Fig. 5 shows that the SOC boundaries of 10 % and 90 % are not violated.

4. CONCLUSION AND OUTLOOK

With the increasing number of globally installed BESS their performance among their whole life cycle becomes increasingly relevant. Operating a BESS under consideration of aging effects minimizes the overall impact of aging and capacity fade in an inhomogeneous

Table 1. Exemplary parameter set for the MPC framework to obtain the results in section 3.2

prediction horizon	4 hours	
control horizon	2 hours	
power demand profile	FCR, 21 days	
objective function	minimize: $\sum_{t=0}^{n} \text{capacity\_loss}_A(t) + \sum_{t=0}^{n} \text{capacity\_loss}_B(t)$	
chemistry	$LiFePO_4$/graphite cell	
aging functions	$Q_{\text{loss, cal}}(\%) = k_{\text{temp, cal}} \cdot k_{\text{SOC}} \cdot \sqrt{t}$ $Q_{\text{loss, cyc}}(\%) = k_{\text{temp, cyc}} \cdot k_{\text{C-rate}} \cdot k_{\text{DOC}} \cdot \sqrt{\text{FEC}}$	
	String A	**String B**
nameplate capacity in kWh	6000	6000
SOC	90 %	40 %
SOH	100 %	85 %

system. For balancing aging effects throughout the entire system and therefore overcome inhomogeneities across the individual sub-units, this work presents a model predictive control framework. By simulating a system behaviour for a specific use case with an according demand profile, the optimal operation strategy can be derived. This work uses the application of frequency containment reserve as an input profile for optimization. A MILP model is presented to determine the optimal operation strategy of a BESS system with two heterogeneous strings considering their calendar and cyclic capacity loss based on LFP battery strings. The MPC framework aims for minimal capacity losses across the whole system in order to minimize the overall capacity fade. The strings' heterogeneous levels in SOH in this work represent the integration of SLB with lower starting SOH into the BESS system. A balanced degradation in that context implies that the operation strategy of a Second Life-BESS avoids the repeated replacement of degraded sub-units. The opposite strategy would be a intended repeated replacement of sub-units that were specifically stressed in operation to conserve the capacity of other sub-units.

The results show that a system setup consisting of sub-units with different aging states (levels of SOH) and their balanced operation is possible. The framework successfully combines two strings with different levels of SOH and optimizes their interaction. It shows that sub-units of different characteristics can be integrated and efficiently operated in a system. The load is shared between the two strings whilst keeping the system‘s total capacity loss as low as possible. In the simulation case study presented in this contribution, the optimizer ”sacrifices” string B by pushing it towards a higher SOC level than string A in order to preserve the new string A.

The optimizer needs further development regarding the consideration of power-dependent inverter losses, which currently make it difficult to precisely fulfil the demand profile. In future work we plan to set the maximization of overall operation time as an objective function in order to adapt the optimization problem towards a total system's RUL maximization. Furthermore we plan to extend the inhomogeneity of strings towards integrating different cell chemistries (thus meaning different aging characteristics). Additionally we intend to perform a simulation series with varying operational temperatures.

AUTHORS' CONTRIBUTIONS

Melina Graner: Conceptualization, Investigation, Methodology, Optimizer, Visualization, Writing – original draft, Writing – review & editing. **Vivek Teja Tanjavooru**: Optimizer, Writing – review & editing. **Andreas Jossen**: Supervision, Writing – review & editing. **Holger Hesse**: Methodology, Funding acquisition, Supervision, Writing – review & editing.

ACKNOWLEDGMENTS

This research is funded by the Bayerische Forschungsstiftung (BFS) via the research project KI-M-Batt (grant number AZ-1563-22).

REFERENCES

[1] Jan Figgener, Peter Stenzel, Kai-Philipp Kairies, Jochen Linßen, David Haberschusz, Oliver Wessels, Georg Angenendt, Martin Robinius, Detlef Stolten, and Dirk Uwe Sauer. The development of stationary battery storage systems in Germany – a market review. Journal of Energy Storage, 29:101153, 2020.

[2] Margaret Mann, Susan Babinec, and Vicky Putsche. Energy storage grand challenge: Energy storage market report, 2020.

[3] Brian Mirletz, Laura Vimmerstedt, Tyler Stehly, Sertac Akar, Dana Stright, Chad Augustine, Philipp Beiter, Stuart Cohen, Wesley Cole, Patrick Duffy, David Feldman, Pieter Gagnon, Parthiv Kurup, Caitlin Murphy, Vignesh Ramasamy, Jarett Zuboy, Gbadebo Oladosu, Jeffrey Hoffmann, Annika Eberle, Owen Roberts, Daniel Mulas Hernando, Greg Avery, Evan Rosenlieb, Anna Schleifer, Dayo Akindipe, and Eric Witter. 2023 annual technology baseline (atb) cost and performance data for electricity generation technologies, 2023.

[4] J. Vetter, P. Novak, M. R. Wagner, C. Veit, K.-C. Moller, J. O. Besenhard, M. Winter, M. Wohlfahrt-Mehrens, C. Vogler, and A. Hammouche. Ageing mechanisms in lithium-ion batteries. Journal of Power Sources, 147(1-2):269–281, 2005.

[5] Xuebing Han, Languang Lu, Yuejiu Zheng, Xuning Feng, Zhe Li, Jianqiu Li, and Minggao Ouyang. A review on the key issues of the lithium ion battery degradation among the whole life cycle. eTransportation, 1:100005, 2019.

[6] Jacqueline S. Edge, Simon O'Kane, Ryan Prosser, Niall D. Kirkaldy, Anisha N. Patel, Alastair Hales, Abir Ghosh, Weilong Ai, Jingyi Chen, Jiang Yang, Shen Li, Mei-Chin Pang, Laura Bravo Diaz, Anna Tomaszewska, M. Waseem Marzook, Karthik N. Radhakrishnan, Huizhi Wang, Yatish Patel, Billy Wu, and Gregory J. Offer. Lithium ion battery degradation: what you need to know. Physical Chemistry Chemical Physics, 23(14):8200–8221, 2021.

[7] Guannan He, Rebecca Ciez, Panayiotis Moutis, Soummya Kar, and Jay F. Whitacre. The economic end of life of electrochemical energy storage. Applied Energy, 273:115151, 2020.

[8] Nils Collath, Benedikt Tepe, Stefan Englberger, Andreas Jossen, and Holger Hesse. Aging aware operation of lithium-ion battery energy storage systems: A review. Journal of Energy Storage, 55:105634, 2022.

[9] Maik Naumann, Cong Nam Truong, Michael Schimpe, Daniel Kucevic, Andreas Jossen, and Holger C. Hesse. Simses: Software for techno-economic simulation of stationary energy storage systems. In International ETG Congress 2017, pages 1–6, 2017.

[10] Stefan Englberger, Andreas Jossen, and Holger Hesse. Unlocking the potential of battery storage with the dynamic stacking of multiple applications. Cell Reports Physical Science, 1(11):100238, 2020.

[11] Matthieu Dubarry, Nicolas Vuillaume, and Bor Yann Liaw. From li-ion single cell model to battery pack simulation. Control Applications, 2008. CCA 2008. IEEE International Conference on Control Applications, 186(2):708–713, 2008.

[12] Sebastian Paul, Christian Diegelmann, Herbert Kabza, and Werner Tillmetz. Analysis of ageing inhomogeneities in lithium-ion battery systems. Journal of Power Sources, 239:642–650, 2013.

[13] Mohammed Khalifa Al-Alawi, James Cugley, and Hany Hassanin. Techno-economic feasibility of retired electric-vehicle batteries repurpose/reuse in second-life applications: A systematic review. Energy and Climate Change, 3:100086, 2022.

[14] Martin F. Börner, Moritz H. Frieges, Benedikt Spath, Kathrin Sputz, Heiner H. Heimes, Dirk Uwe Sauer, and Weihan Li. Challenges of second-life concepts for retired electric vehicle batteries. Cell Reports Physical Science, 3(10):101095, 2022.

[15] Council of the European Union, Council adopts new regulation on batteries and waste batteries, 2023.

[16] Lluc Canals Casals, B. Amante Garcia, and Camille Canal. Second life batteries lifespan: Rest of useful life and environmental analysis. Journal of environmental management, 232:354–363, 2019.

[17] Narjes Fallah and Colin Fitzpatrick. How will retired electric vehicle batteries perform in grid-based second-life applications? a comparative techno-economic evaluation of used batteries indifferent scenarios. Journal of Cleaner Production,

361:132281, 2022.

[18] Xiaosong Hu, Xinchen Deng, Feng Wang, Zhongwei Deng, Xianke Lin, Remus Teodorescu, and Michael G. Pecht. A review of second-life lithium-ion batteries for stationary energy storage applications. Proceedings of the IEEE, 110(6):735–753, 2022.

[19] Daniel Kucevic, Benedikt Tepe, Stefan Englberger, Anupam Parlikar, Markus Mühlbauer, Oliver Bohlen, Andreas Jossen, and Holger Hesse. Standard battery energy storage system profiles: Analysis of various applications for stationary energy storage systems using a holistic simulation framework. Journal of Energy Storage, 28:101077, 2020.

[20] Maik Naumann, Michael Schimpe, Peter Keil, Holger C. Hesse, and Andreas Jossen. Analysis and modeling of calendar aging of a commercial lifepo4/graphite cell. Journal of Energy Storage, 17:153–169, 2018.

[21] Maik Naumann, Franz B. Spingler, and Andreas Jossen. Analysis and modeling of cycle aging of a commercial lifepo4/graphite cell. Journal of Power Sources, 451:227666, 2020.